Electronic Supplementary Material (ESI) for Energy & Environmental Science.
This journal is © The Royal Society of Chemistry 2023

# Supporting Information

# For

# Self-powered Recycle of Spent Lithium Iron Phosphate Batteries *Via* Triboelectric Nanogenerator

*Baofeng Zhang,[a,b] Lixia He,[a,b] Jing Wang,[a,b] Yuebo Liu,[a,d] Xu Xue,[e] Shengnan He,[e] Chuguo Zhang [a,b,] Zhihao Zhao,[a,b] Linglin Zhou,[a,b] Jie Wang,[*a,b,d] Zhong Lin Wang[a,c]*

[a] Beijing Institute of Nanoenergy and Nanosystems, Chinese Academy of Sciences, Beijing 100083, P. R. China
[b] College of Nanoscience and Technology, University of Chinese Academy of Sciences, Beijing 100049, P. R. China
[c] Georgia Institute of Technology, Atlanta, GA 30332, USA
[d] Center on Nanoenergy Research, School of Physical Science and Technology, Guangxi University, Nanning, 530004, P. R. China
[e] Institute of Science and Technology for New Energy, Xi'an Technological University, Xi'an 710021, China

**Corresponding Authors**

*E-mail: wangjie@binn.cas.cn

**Note S1. The Working Mechanism of TENG**

With the mechanism of contact electrification, PA layer is positively charged and Cu exhibits negatively when contact (**Figure S2a**). As the PA layer slides from the left to the right, the electrons on the left Cu electrode will transfer to the right one (**Figure S2b**) till it overlaps with the Cu layer (**Figure S2c**). Later, when another PA film reaches the left Cu layer, the electrons on the right Cu electrode return to the right electrode (**Figure S2d**). Therefore, an alternative signal is generated in the outside circuit.

**Note S2. Activation Energy Calculation According to The Arrhenius Formula**

The main factors affecting the leaching efficiency are as follows: (1) diffusion of reactive ions within the liquid film, (2) diffusion of reactive ions through the product layer of the particles up to the surface of the inner core, and (3) the chemical reaction at the surface of inner core. The leaching kinetic model can be divided into three types: (1) Surface chemical control model (Equation 1),[1] (2) Diffusion control model (Equation 2),[2] (3) Log rate law model (Equation 3),[3]

$$1-(1-x)^{1/3} = k_1 t \quad (1)$$

$$1-2/3x-(1-x)^{2/3}=k_2 t \quad (2)$$

$$(-\ln(1-x))^2=k_3 t \quad (3)$$

where $x$ is leaching efficiency (%); $k_1$, $k_2$ and $k_3$ represent the different reaction rate constant ($min^{-1}$); and $t$ refers to the leaching time (min). The leaching efficiency data of each metal was used to fit the above three formulas respectively under different experimental conditions.

The activation energy of each metal was obtained by Arrhenius equation (Wu et al.,2019) (Eq. (4))

$$\ln k = \ln A - Ea/\mathrm{RT} \quad (6)$$

where $A$ is the frequency factor; $Ea$ represents the apparent activation energy; R is the gas constant of 8.3145 J/KÆmol; and $T$ (k) is the leaching temperature.

**Note S3. Li-ion Diffusion Coefficient of The Regenerated LFP**

If the charge transfer at the interface is fast enough and the rate limiting step is the lithium diffusion in electrode, the relationship of the peak current and the CV sweep rate is:

$$ip = (2.69 \times 10^5) n^{3/2} A D_{Li}^{1/2} C_{Li} v^{1/2} \quad (1)$$

where $ip$ is the peak current (A), $^{n}$ is the charge-transfer number, $^{A}$ is the contact area between LFP and electrolyte (here the geometric area of electrode, 2 $cm^2$, is used for simplicity), $C_{Li}$ is the concentration of lithium ions in the cathode, and $v$ is the potential scan rate (V $s^{-1}$).

**Note S4. Detailed Information for The Cost Assessment of Spent LFP Battery**

For the cost assessment of spent LFP battery, consistency and authority are two important aspects to evaluate the cost of raw material, reagents, products, and energy consumptions. In order to better compare out work with previous works, we cited two works below (ref.4 and ref.5) for the prices of the parts of the materials. For the material or the reagent that did not use before, we checked the price in "Alibaba.com".

Taking 1.0 kg of spent LFP batteries as an example, the economic assessment for spent LFP battery recovery is performed based on our proposed process. The details are as follows (1$ = 6.8 RMB):

**i) The separation of LFP pouch battery**: 446.7g LFP cathode electrode, 256.5g graphite anode, 90.9 g casing, and 25.3 g separator are obtained after a manual dismantling and sorting process. The input cost of 1.0 kg spent LFP battery is $2.326,[4] and the profits from the casing and separators, graphite are $0.023 and $0.180, respectively.

**ii) Electrochemical Recycling of LFP cathode material:** NMP (500 mL) is used to dissolve the binder and the obtained LFP cathode material and aluminum foil are 416.1g and 30.6g. Then LFP cathode material is mixed in 1L NaCl solution for anodic oxidation, and 198.8g $Na_2CO_3$ is added to precipitate $Li^+$ in the solution. The obtained $Li_2CO_3$ and $FePO_4$ are 97.3g and 397.2g, while the hydrogen obtained in the cathode is 29.3L. Therefore, the input cost of NMP, NaCl, and $Na_2CO_3$ is $1.60, $0.015 and $0.048. While the profits from the aluminum foil, and hydrogen are $0.009, $0.023, respectively.

The operation time for the recycle of LFP is about 2h. The motor for the electrochemical recycling technology is 0.1k W. The input cost of electricity for 1.0 kg of spent LFP battery recycling was 2h x 0.1 kW x $0.07/kWh = $0.014.

**iii) The generation of LFP**: extra 1.0% $Li_2CO_3$ (0.972g, $0.011), 10 L nitrogen ($0.29) and 0.38 kWh electricity ($0.027) is input to obtain 416.0 high-performance cathode material ($5.811).

Thus, the total cost ($C_{total}$) and profit ($P_{total}$) of whole process for regeneration of LFP cathode material can be calculated below.

$$C_{total} = raw\ material + reagents + energy = \$2.326 + \$1.964 + \$0.041 = \$4$$

$$P_{total} = new\ LFP + reagents + hydrohen = \$5.811 + 0.212 + 0.023 = \$6.046$$

In summary, the total profit of whole process is \$1.715 when dealing with 1.0 kg of spent LFP batteries. Where, for the cost part, the raw material is spent LFP batteries. reagents are NMP, NaCl, and $Na_2CO_3$, extra $Li_2CO_3$, nitrogen. Energy is the electricity needed for separation and regeneration of LFP. For the profit part, reagents are the casing and separators, graphite, aluminum foil.

It is notable that the NMP can be repeatedly use to dissolve the cathode material after a distillation process. And we assume that the attrition rate is 10% when distilling. Thus, the total cost can be saved 90% of the cost of the NMP from \$4.331 to \$2.891. The profit can be enhanced from \$1.715 to \$3.155.

The prices for the parts are as follows: spent LFP battery (\$2.326/kg), spent LFP cathode material (\$0.306/kg), graphite anode material (\$0.7/kg), spent casing/separator (\$0.2/kg), new separator (\$18.2/kg), new aluminum-plastic film (\$18.2/kg), electrolyte (\$5.51/kg), hydrogen (\$8.82/kg), Cu foil (\$7.0/kg), NMP (\$3.2/kg), NaCl (\$0.015/kg), acid (\$0.05/kg), $Na_2CO_3$ (\$0.24/kg), Al foil (\$0.3/kg), $Li_2CO_3$ (\$11.5/kg), FP precursor (\$1.0/kg), nitrogen (\$29.4/$m^3$), electricity (\$0.07/kWh), new LFP cathode material (\$13.97/kg).

**Note S5. Detailed Information for The Cost Assessment of Direct recycling**

We take the "A recrystallization approach to repairing spent $LiFePO_4$ black mass, J. Mater. Chem. A,2023, 11, 9057" as a case study to investigate the cost assessment of direct recycling.[5] The repairing procedure are as follows,

1 g of the spent LFP powder was mixed with 0.08 g $LiNO_3$ and 0.02 g anhydrous glucose (AR) by ball-milling at 300 rpm for 30 min, noted as the mixture. Then the powder mixture was placed inside an alumina porcelain boat and then heated in a muffle furnace at 300 $^oC$ and maintained for 30 min in air (this process may release nitric oxides such as $NO_2$, and the tail gas should be filtered by using an alkaline solution). The LFP powder which was just heated was quickly quenched by pouring ~10 ml of DI water into the porcelain boat, and washed with DI water and ethanol via suction filtration to remove the unreacted $LiNO_3$ and other solvable residues. Then the powder was placed in a 10 ml centrifuge tube filed with 5 ml saturated $ZnCl_2$ aqueous solution and centrifuged for 5 min at a differential speed of 3000–6000 rpm (peak centrifuge force: ~122 G). Typically, ~0.74 g repaired LFP (~92% of LFP from the black mass) can be collected from the sediment in the centrifuge tube (after washing with DI water to remove residual $ZnCl_2$), and the powder floating on top can be collected as spent graphite.

The main material, reagent, and energy for recycling 1 kg spent LFP batteries in this procedure is listed (supposing the same yield as our work with 447g LFP cathode material when recycling 1kg spent LFP battery):

1. 1kg spent LFP battery, $2.326/kg
2. ~35.76g $LiNO_3$, $33.8/kg
3. ~8.94 g anhydrous glucose, $6.17/kg
4. ~41.5g NaOH in alkaline solution for filtering $NO_2$ ($NaOH/NO_2$=2:1, $0.66/kg,)
5. saturated $ZnCl_2$ ($1.323/kg, solubility, 432g/100g, 21.6g/5mL)
6. yield: 74%,
7. The energy for this procedure is $0.07/kWh

Therefore, the total cost of recycling 1kg spent LFP is material ($2.326) + reagent ($1.209 +$0.055 + $0.027) + energy (~$0.021) without considering the cost of $ZnCl_2$.

The profit is new LFP ($4.621) and spent graphite ($0.081). In summary, the total profit of whole process is $1.06 when dealing with 1.0 kg of spent LFP batteries without considering the cost of $ZnCl_2$. The results also indicate that although the direct recycling is favorable due to the simplified procedure and low energy input, the additives are pricey.

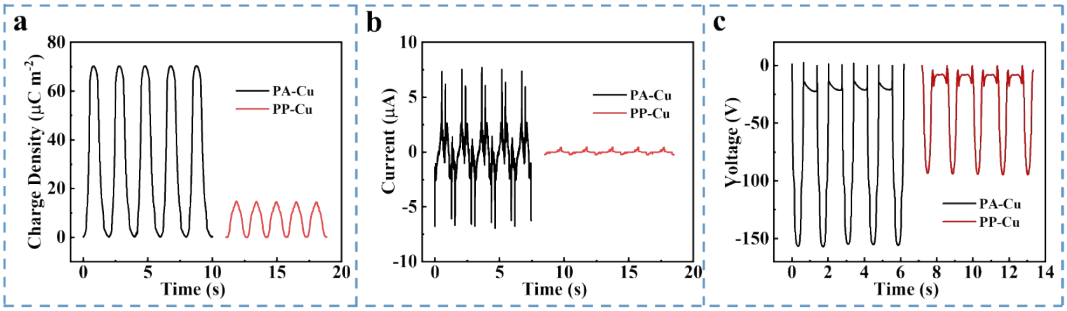


Figure S1. Output performance of PA/Cu pair and PP/Cu pair. (a) The transferred charge, (b) current, and (c) voltage of PA/Cu pair and PP/Cu pair.

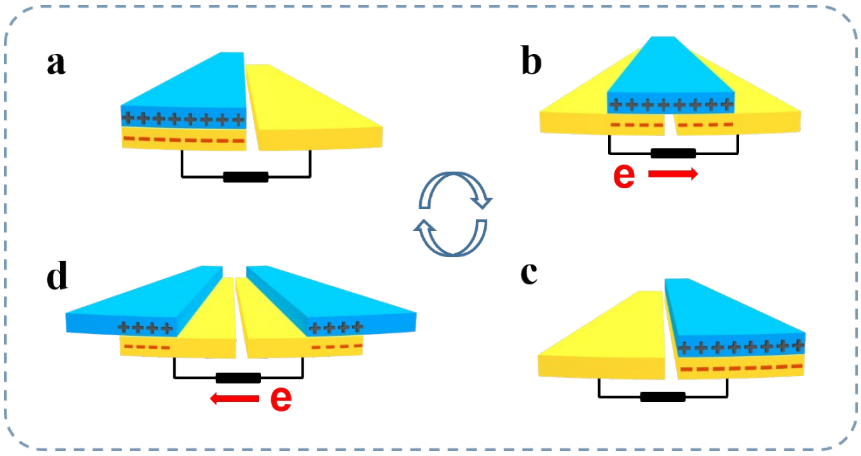


Figure S2. The working mechanism of TENG. (a) The contact of PA and Cu, (b) PA layer slides from the left to the right, (c) PA layer overlaps with the Cu layer, (d) another PA film reaches the left Cu layer.

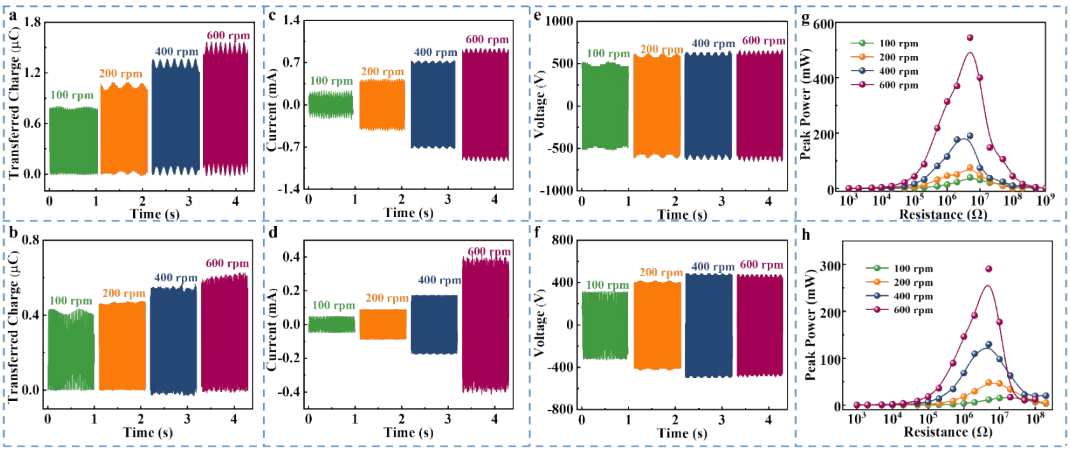


Figure S3. The output of TENG. (a, c, e, g) The transferred charge, current, voltage and peak power of OR-TENG, (b, d, f, h) The transferred charge, current, voltage and peak power of IR-TENG.

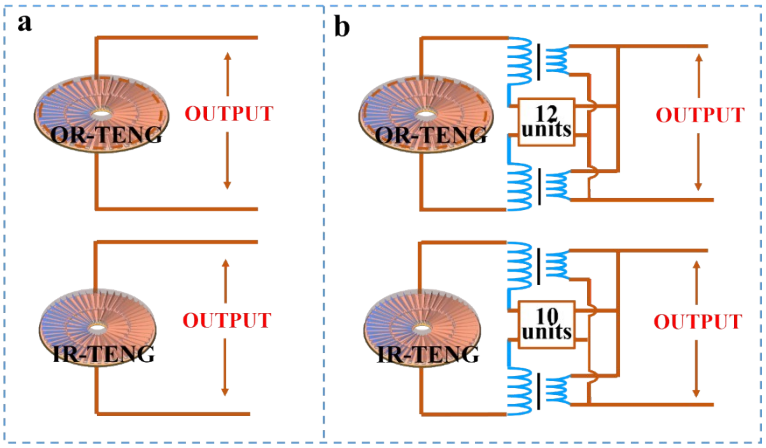


Figure S4. The circuit diagram of TENG. (a) without and (b) with TFs.

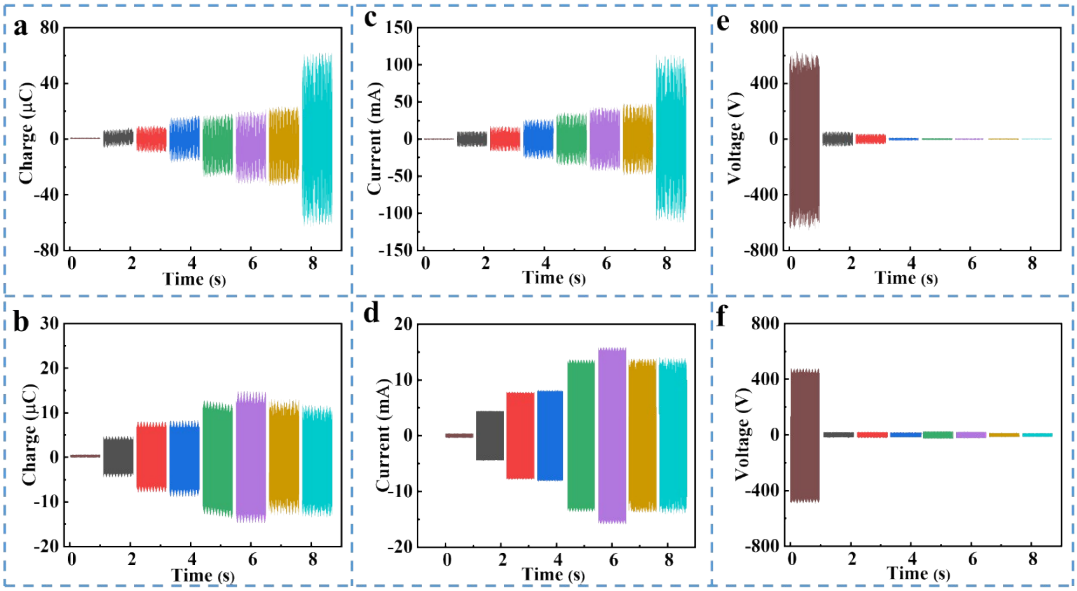


Figure S5. The output of TENG rectified with TFs. (a) The transferred charge, (c) current and (e) voltage of OR-TENG after rectification with TFs, (b) The transferred charge, (d) current and (f) voltage of IR-TENG after rectification with TFs.

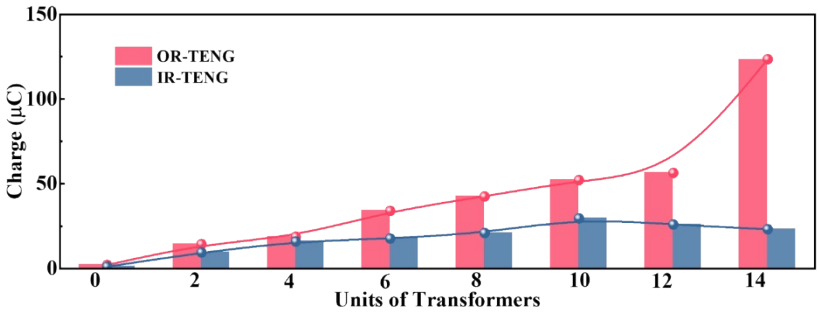


Figure S6. The transferred charge of OR-TENG and IR-TENG after rectification with TFs.

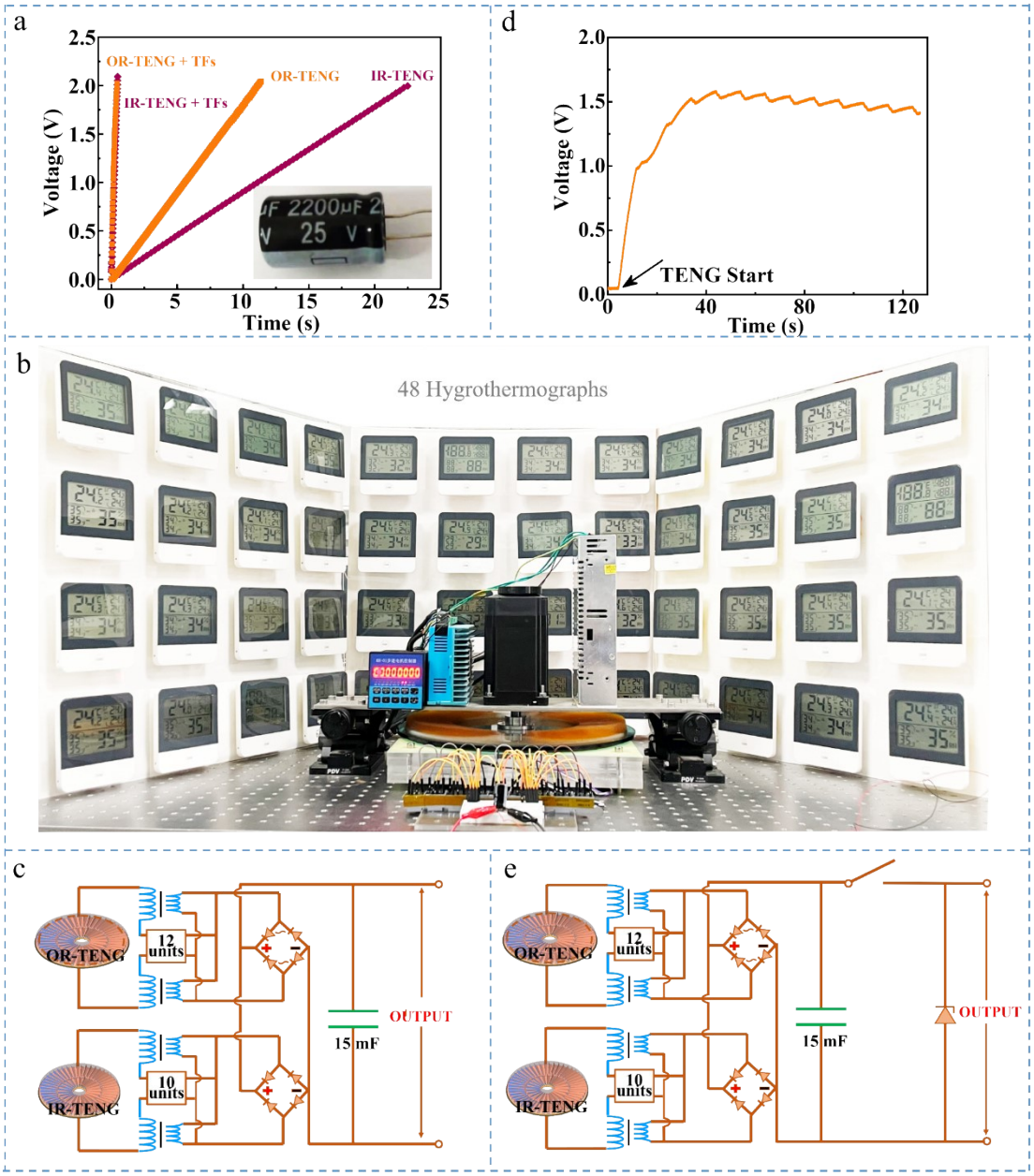


Figure S7. The application of TENG. TENG as a power supply to (a) charge capacitors, (b) 48pcs of hygrothermographs according to (c) the circuit diagram. (d) the voltage of the hygrothermographs powered by TENG and the (e) the circuit diagram of powering a wireless temperature and humidity sensor (T & H sensor), a wireless vibration sensor and a wireless light sensor.

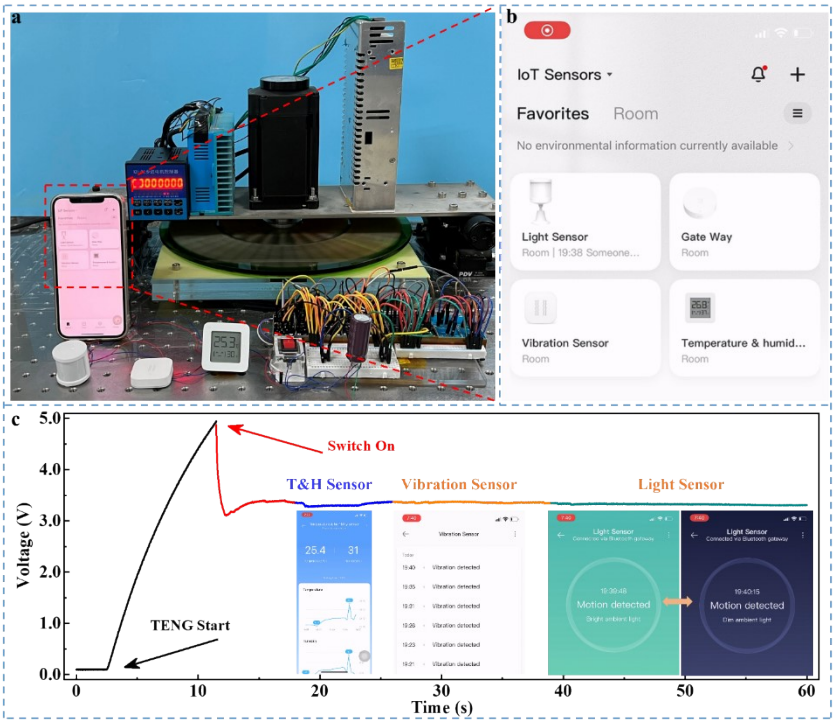


Figure S8. The application of TENG. The fabricated TENG powers (a) a wireless temperature and humidity sensor, a wireless vibration sensor and a wireless light sensor. (b) The App of the sensors and (c) the working conditions when driving the relevant sensors.

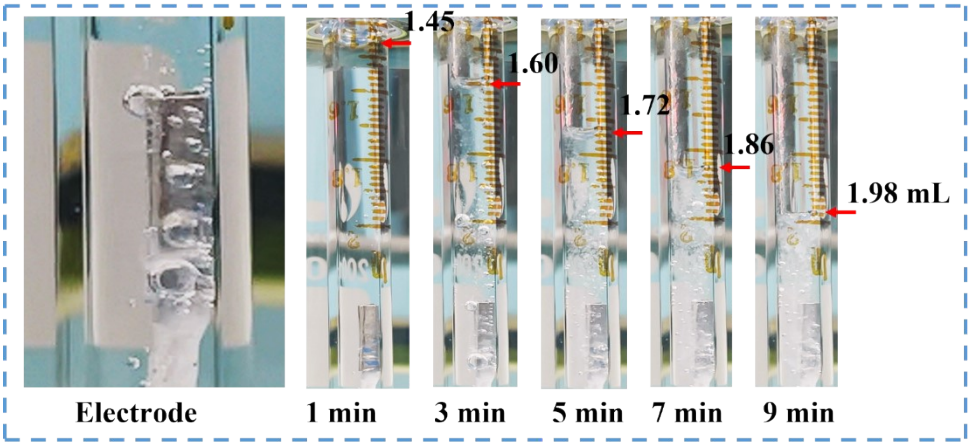


Figure S9. The generation of hydrogen in the cathode.

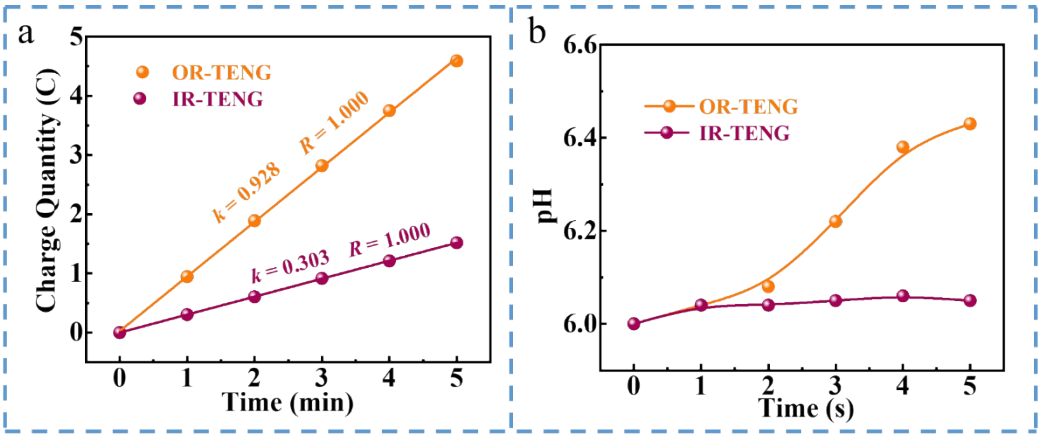


Figure S10. The working conditions of electrochemical reactor. (a) The quantity of transferred charge and (b) pH varies with time.

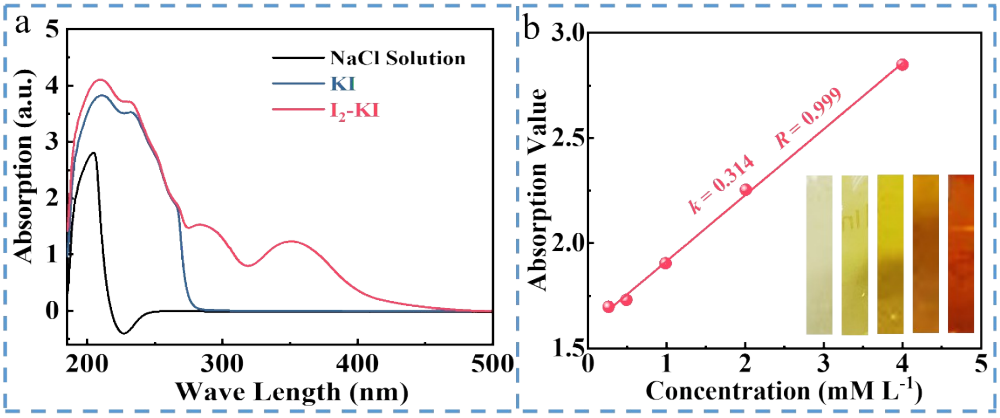


Figure S11. UV-Vis spectra test. (a) UV-Vis spectra of NaCl, KI and $I_2$-KI solution and (g) the standard curve of KI solution for calibrating $ClO^-$ concentration.

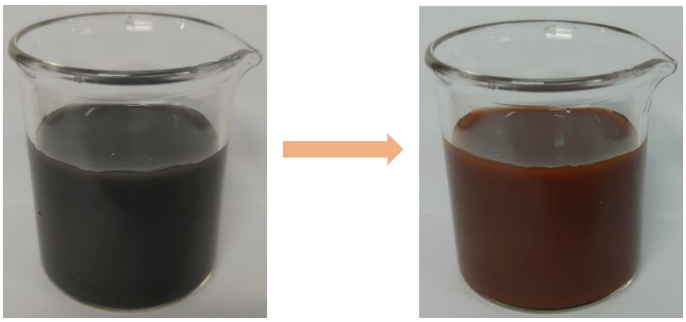

Figure S12. The color of the electrochemical leaching under 0.7 mol $L^{-1}$ NaClO in 1 hour.

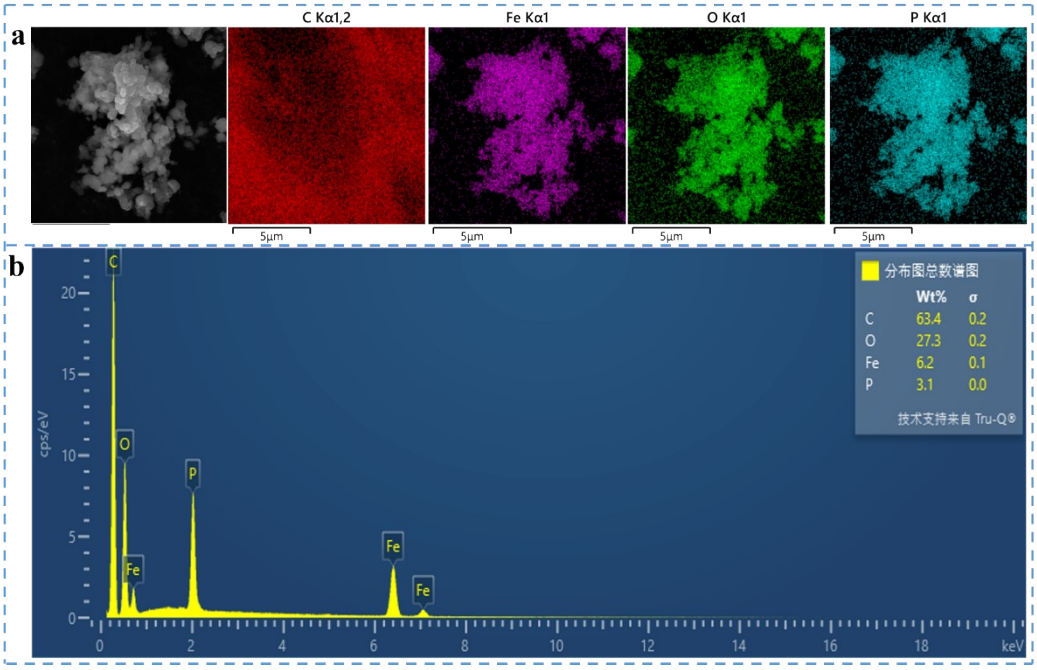


Figure S13. The characterization of regenerated LFP cathode material. (a) SEM of the regenerated LFP cathode material and the (b) energy dispersive x-ray (EDX) test.

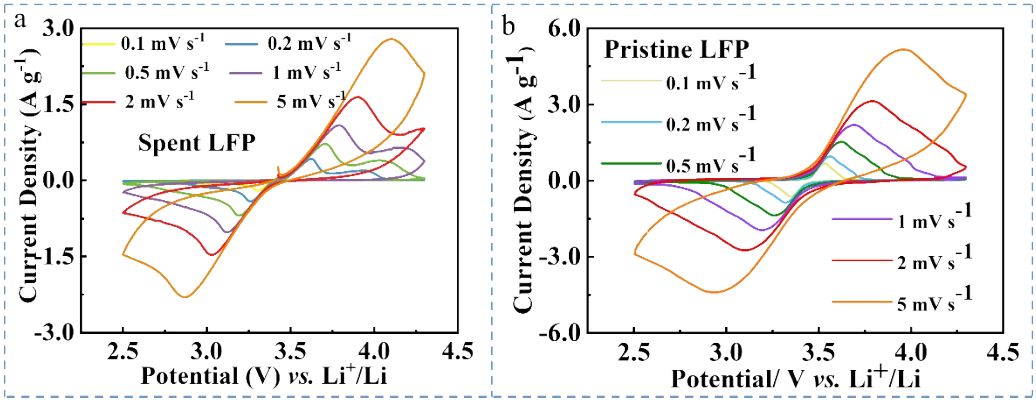


Figure S14. CV curves of samples at different scanning rates. (a) spent LFP and (b) pristine LFP.

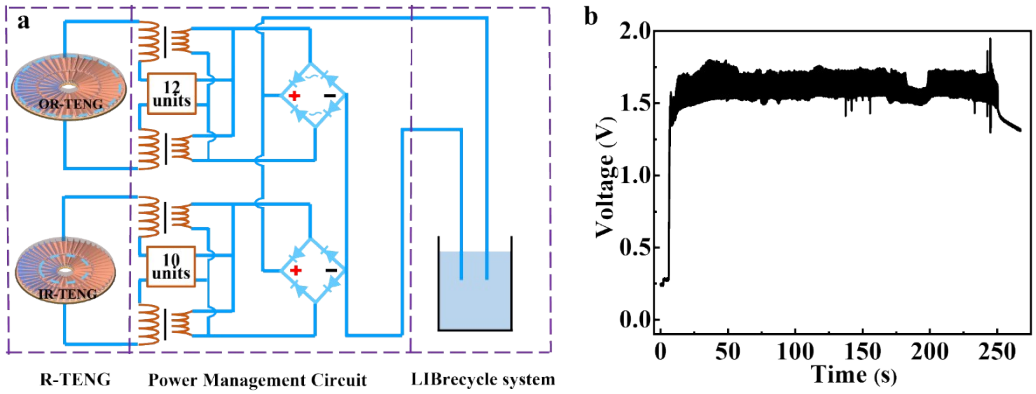


Figure S15. The working conditions of fabricated self-powered spent LIB recovery system. (a) The circuit diagram of self-powered LIBs recycle system and (b) the voltage of the electrochemical LIB reactor.

Table S1. The summary of LFP cathode materials recycled from spent LIBs in the literature and this study.

| Item | Recycling methods | Procedure | Material consumption | Performance | Energy Input | Reference |
|---|---|---|---|---|---|---|
| 1 | Direct regeneration | Solution relithiation treatment (180 °C 5h), annealing (600 °C 2h) | LiOH, citric acid, $Li_2CO_3$ | 162,144, 102 mAh $g^{-1}$ at 0.2, 2, and 10 C | Yes | [6] |
| 2 | Direct regeneration | Relithiation in Ar (300 °C 6 h), annealing in Ar (600 °C for 6 h) | $LiNO_3$, $FeC_2O_4$, sucrose, | 145 mAh $g^{-1}$ at 0.5 C | Yes | [7] |
| 3 | Direct regeneration | Sintered in Ar/$H_2$ (800 °C for 6 h) | $Li_2$DHBN, | 127 (2C), 111 (5C) , 97 (10C) mAh $g^{-1}$ at 2, 5, 10 C, 90% at 1 C after 300 cycles | Yes | [8] |
| 4 | Electrochemical Regeneration | Preparing prelithiation Separator | $Li_2C_2O_4$, CMK-3, PVDF, PP separator, | 159.0 (0.1C),161.4 (0.2C), 158.4 (0.5C),139.4 (1C) mAh $g^{-1}$, 90.7% after 292 cycles | Yes | [9] |
| 5 | Direct regeneration | Heating (300 °C, 30min), | Glucose, $LiNO_3$, alkaline solution | 162 mAh $g^{-1}$ at 1C, 97% at 0.5 C after 500 cycles | Yes | [5] |

| | | | | | | |
|---|---|---|---|---|---|---|
| 6 | Direct regeneration | Hydrothermal treatment (180 °C 5h), sintered in argon (700 °C for 5 h) | Ethanol, PVP, $CH_3COOLi$ | 146 mAh $g^{-1}$ at 0.3 C, 95.7% at 0.5 C after 230 cycles | Yes | [10] |
| 7 | Direct regeneration | Hydrothermal treatment (200 °C 3h), sintered in argon (700 °C for 2 h) | LiOH, tartaric acid | 165.9 (0.1C), 151.9 (0.5C), 145.9 (1C), 133.1 (2C) and 114.9 (5C) mAh $g^{-1}$, 99.1% after 200 cycles at 1 C | Yes | [11] |
| 8 | Electrochemical regeneration | Discharging, annealing (600 °C 2h) | $Li_2SO_4$ | 147.5 (0.1C),150.0 (0.2C), 124.7 (2C), 70.6 (10C) mAh $g^{-1}$, 95.30% and 84.68% after 500 cycles at 1C and 5C. | Yes | [12] |
| 9 | Oxidation leaching | oxidation leaching, thermal annealing at 350 °C for 1 h, calcinated at 650 °C for 10 h in argon | $H_2O_2$, LiOH, citric acid | 144 (1C), 133 (5C), 120 (10C) mAh $g^{-1}$, 99.0 % after 300 cycles at 5C. | Yes | [13] |
| 10 | Electrochemical regeneration | Electrochemical separation, annealing at 350 °C for 2 h, | NaCl $Li_2CO_3$ | 167.8 mAh $g^{-1}$ (0.1C), 161.1 mAh $g^{-1}$ (0.2C), | Partly powered by | This Work |

| | | | | | | |
|---|---|---|---|---|---|---|
| | | sintered at 650 ℃ for 6 h | | (1C), 142.4 mAh $g^{-1}$<br>(2C), 125.5 mAh $g^{-1}$<br>(5C), 108.6 mAh $g^{-1}$<br>(10C), 94.0 % after 300 cycles at 5C. | fabricated TENG. | |

## Reference


1. L. Zhuang, C. Sun, T. Zhou, H. Li and A. Dai, *Waste Manage. (Oxford)*, 2019, **85**, 175-185.
2. Y. Chen, D. Chang, N. Liu, F. Hu, C. Peng, X. Zhou, J. He, Y. Jie, H. Wang, B. P. Wilson and M. Lundstrom, *JOM*, 2019, **71**, 4465-4472.
3. X. Zhang, H. Cao, Y. Xie, P. Ning, H. An, H. You and F. Nawaz, *Sep. Purif. Technol.*, 2015, **150**, 186-195.
4. Y. Song, B. Xie, S. Song, S. Lei, W. Sun, R. Xu and Y. Yang, *Green Chem.*, 2021, **23**, 3963-3971.
5. Z. Wang, H. Xu, Z. Liu, M. Jin, L. Deng, S. Li and Y. Huang, *J. Mater. Chem. A*, 2023, **11**, 9057-9065.
6. P. Xu, Q. Dai, H. Gao, H. Liu, M. Zhang, M. Li, Y. Chen, K. An, Y. S. Meng, P. Liu, Y. Li, J. S. Spangenberger, L. Gaines, J. Lu and Z. Chen, *Joule*, 2020, **4**, 2609-2626.
7. X. Liu, M. Wang, L. Deng, Y.-J. Cheng, J. Gao and Y. Xia, *Industrial & Engineering Chemistry Research*, 2022, **61**, 3831-3839.
8. G. Ji, J. Wang, Z. Liang, K. Jia, J. Ma, Z. Zhuang, G. Zhou and H.-M. Cheng, *Nat. Commun.*, 2023, **14**, 584.
9. M. Fan, Q. H. Meng, X. Chang, C. F. Gu, X. H. Meng, Y. X. Yin, H. L. Li, L. J. Wan and Y. G. Guo, *Adv. Energy Mater.*, 2022, **12**, 2103630.
10. K. Jia, J. Ma, J. Wang, Z. Liang, G. Ji, Z. Piao, R. Gao, Y. Zhu, Z. Zhuang, G. Zhou and H.-M. Cheng, 2023, **35**, 2208034.
11. B. Chen, M. Liu, S. Cao, H. Hu, G. Chen, X. Guo and X. Wang, *J. Alloys Compd.*, 2022, **924**, 166487.
12. D. Peng, X. Wang, S. Wang, B. Zhang, X. Lu, W. Hu, J. Zou, P. Li, Y. Wen and J. Zhang, *Green Chem.*, 2022, **24**, 4544-4556.
13. X. Qiu, B. Zhang, Y. Xu, J. Hu, W. Deng, G. Zou, H. Hou, Y. Yang, W. Sun, Y. Hu, X. Cao and X. Ji, *Green Chem.*, 2022, **24**, 2506-2515.